PQ Theory-Based Control of Single-Stage V2G Three-Phase BEV Charger for High-Voltage Battery

Rachid, Aziz; Fadil, Hassan El; Koundi, M.; Idrissi, Z. El; Tahri, A.; Giri, Fouad; Guerrero, J. M.

Published in:
IFAC-PapersOnLine

DOI (link to publication from Publisher):
10.1016/j.ifacol.2019.12.624

Publication date:
2019

Document Version
Publisher's PDF, also known as Version of record

Available online at www.sciencedirect.com

ScienceDirect

IFAC PapersOnline CONFERENCE PAPER ARCHIVE

IFAC PapersOnLine 52-29 (2019) 73–78

PQ Theory-Based Control of Single-Stage V2G Three-Phase BEV Charger for High-Voltage Battery

Aziz Rachid*, Hassan El Fadil*, M. Koundi*, Z. El Idrissi, A. Tahri*, Fouad Giri, J. M. Guerrero*****

**ESIT Team, LGS Laboratory, ENSA, Ibn Tofail University, 14000, Kénitra, Morocco.*
(e-mail: rachidaziz03@gmail.com; elfadilhassan@yahoo.fr; mohamed.koundi.mk@gmail.com; zakariae.elidrissi@gmail.com; abdelouahadtahri@yahoo.fr)
***Laboratoire d'Automatique de Caen, Université de Caen, Bd Marechal Juin, B.P 8156, 14032, Caen*
(e-mail : fouadgiri@yahoo.fr)
****Department of Energy Technology, Aalborg University, 9220 Aalborg East, Denmark*
(e-mail: joz@et.aau.dk)

Abstract: This work dealt with a modeling and a PQ theory-based control of a vehicle-to-grid (V2G) three-phase battery electric vehicle (BEV) charger. This studied system consists of a bidirectional ac-dc three-phase power converter associated with an EV battery pack via an LC filter. The control of the studied system is performed in order to meet all control objectives, namely : (i) Guaranteeing a unity power factor (UPF) during the grid-to-vehicle (G2V) operating mode; (ii) Regulating the reactive power injected during the V2G operating mode; and (iii) Ensuring the battery charging and the battery discharging, safely. To achieve all these objectives, a backstepping controller using the PQ theory has been designed. Therefore, an imbricate-loops structure has been adopted to regulate the reactive power injected into the power grid and to ensure the charging and discharging of the battery. The achievement of all the objectives of the proposed nonlinear controller was confirmed by numerical simulations performed using the MATLAB/Simulink software.

Keywords: BEV charger, Bidirectional three-phase ac-dc power converter, Nonlinear control, Backstepping-based controller, PQ theory, V2G charger, V2X technology.

1. INTRODUCTION

Nowadays, energy storage is one of the fundamental axes of international treaties on climate and energy. Much of the renewable energy is already produced, but the storage of this energy hardly takes place. Therefore, by intelligently addressing the issue of storing clean and renewable solar and wind energy, we can accelerate the transition to a zero-emissions world without major investments in the power grid. In this matter, the electric vehicle (EV) can play a very large role. Indeed, due to the vehicle-to-everything (V2X) technology, the EV can now be used to temporarily store energy, but also to restore it later (Rachid et al., 2019a). For example, we can power the home in the evening by using the EV battery while during the day we can recharge the EV battery with the office's solar panels. Truthfully, V2X is a collective concept which means that the energy can not only be returned to the power grid (i.e. the vehicle-to-grid (V2G) operating mode), but also to the home electrical installation (i.e. the vehicle-to-home (V2H) operating mode) or e.g. at the camping (i.e. the vehicle-to-live (V2L) operating mode) (Rachid, El Fadil & Giri, 2018). To ensure this functionality, namely bidirectional charging, EVs are equipped with so-called V2X battery chargers that can allow the electrical energy to flow in both directions: from the power grid to the battery (i.e. the charging mode: Grid-to-Vehicle (G2V)) as well as from the battery to the power grid (i.e. V2G discharging mode) (Rachid et al., 2017).

In the last two decades, various topologies have been proposed to best meet the requirements for V2X technology. Thus, many structures of the bidirectional chargers have emerged: onboard or offboard, conductive or inductive, dedicated or integrated, single-stage or dual-stage which can be supplied by single-phase or three-phase power grid (Mahmud et al., 2018; Rubino, Capasso & Veneri, 2017; Yilmaz & Krein, 2013).

In this work, we propose a single-stage V2G three-phase BEV charger with a rated power of 22KW. It consisting of a single ac-dc power converter acting as a power factor controller (PFC) and ensuring the battery charging and the battery discharging during the G2V mode and V2G mode, respectively. The injected reactive power regulation is also guaranteed by the control and management unit (CMU) (Buja, Bertoluzzo & Fontana, 2017). The diagram block of the whole studied system is illustrated by Fig. 1.

The rest of the paper is organized as follows: In section 2 the single-stage V2G three-phase BEV charger is described and modeled; section 3 is devoted to backstepping controller design; in section 4, numerical simulations are carried out in order to illustrate the effectiveness of the proposed controller, and Finally, a conclusion and a reference list end the paper.

10.1016/j.ifacol.2019.12.624

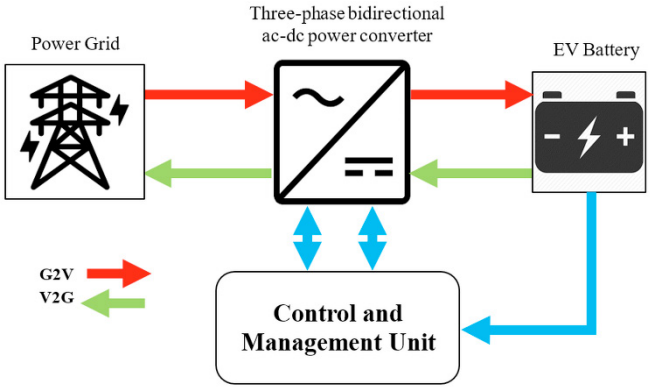

Fig. 1. The diagram block of the studied system

2. SYSTEM OVERVIEW AND MODELLING

2.1 System Overview

The global studied system is a single-stage bidirectional three-phase BEV charger which is able to charge and to discharge EV HV batteries. Its electrical circuit illustrated by Fig. 2 is consisting of a single power converter linked to EV battery via an LC filter. The converter is a bidirectional three-phase ac-dc power converter composed of six current-reversible power switches namely K_1, K_2, K_3, K_4, K_5, and K_6. Each switch is an IGBT mounted upside down with a power-diode to ensure the current-reversibility. The LC filter composed by the capacitor C_{dc} and the coil $\{L_f, r_f\}$ makes it possible to reduce the ripples of the voltage V_{dc} at the output of the converter as well as those of the battery current I_b. In this work, the EV battery is modeled by its equivalent electrical circuit consisting of putting in series two elements: the resistance R_B and the voltage source U_{oc} (Anon, 2017; Mi & Masrur, 2017). R_B is the battery Equivalent Series Resistance (ESR) while U_{oc} represents the battery Open Circuit Voltage (OCV) which is a nonlinear function of the battery State of Charge (SOC) (see Fig. 3). The studied charger is supplied by the three-phase power grid voltages $\{e_1, e_2, e_3\}$ through three smoothing coils $\{L_g, r_g\}$ making it possible to reduce the ripples of the three-phase power grid currents $\{i_1, i_2, i_3\}$. The whole system is controlled by a double three-phase SPWM (Sinusoidal Pulse Width Modulation) switching signals $\{u_1, u_2, u_3\}$ and $\{\bar{u}_1, \bar{u}_2, \bar{u}_3\}$ which are generated by the Control and Management Unit (CMU) (see Fig. 1).

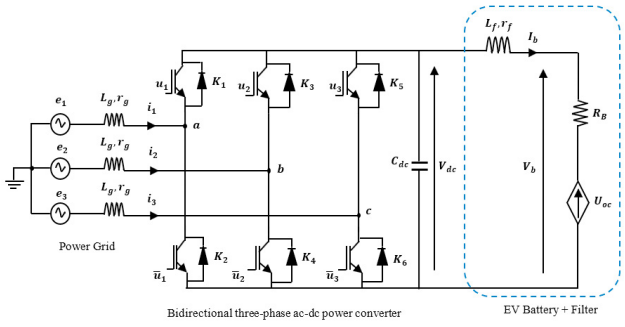

Fig. 2. The electrical circuit of the bidirectional three-phase BEV charger

2.2 System Modelling

For the inspection of Fig. 2 and using Kirchhoff's laws, the following instantaneous model of the whole studied system is obtained(Rachid et al., 2019b)

$$\frac{di_{123}}{dt} = -\frac{r_g}{L_g} i_{123} - \frac{1}{L_g} K u_{123} V_{dc} + \frac{1}{L_g} e_{123} \quad (1a)$$

$$\frac{dV_{dc}}{dt} = \frac{1}{C_{dc}} (u_{123})^t i_{123} - \frac{1}{C_{dc}} I_b \quad (1b)$$

$$\frac{dI_b}{dt} = \frac{1}{L_f} V_{dc} - \frac{(r_f + R_B)}{L_f} I_b - \frac{1}{L_f} U_{oc}(soc) \quad (1c)$$

$$\frac{d(\mathrm{SOC})}{dt} = \frac{I_b}{Q_n} \quad (1d)$$

where $i_{123} = [i_1 \quad i_2 \quad i_3]^t$ are the power grid line currents; $e_{123} = \begin{bmatrix} e_1 \\ e_2 \\ e_3 \end{bmatrix} = \begin{bmatrix} E_m \sin(\omega t) \\ E_m \sin(\omega t - \frac{2\pi}{3}) \\ E_m \sin(\omega t - \frac{4\pi}{3}) \end{bmatrix}$ are the power grid phase-neutral voltages; $K = \frac{1}{3}\begin{bmatrix} 2 & -1 & -1 \\ -1 & 2 & -1 \\ -1 & -1 & 2 \end{bmatrix}$ is a constant matrix; V_{dc} is the dc-bus voltage; I_b is the battery current; U_{oc} is the battery OCV; Q_n is the battery capacity and finally, $u_{123} = [u_1 \quad u_2 \quad u_3]^t$ are the PWM switching signals of the three-phase ac-dc power converter.

In this work, the PQ theory is used to control the active power P and the reactive power Q. To this end, it is more convenient to rewrite the instantaneous model (1a-d) in the αβ coordinates. Therefore, the instantaneous model (1a-e) of the studied system can be easily rewritten in the αβ coordinates as follows

$$\frac{di_{\alpha\beta}}{dt} = -\frac{1}{L_g} r_g i_{\alpha\beta} - \frac{1}{L_g} V_{dc} u_{\alpha\beta} + \frac{1}{L_g} e_{\alpha\beta} \quad (2a)$$

$$\frac{dV_{dc}}{dt} = \frac{1}{C_{dc}} i_\alpha u_\alpha + \frac{1}{C_{dc}} i_\beta u_\beta - \frac{1}{C_{dc}} I_b \quad (2b)$$

$$\frac{dI_b}{dt} = \frac{1}{L_f} V_{dc} - \frac{(r_f + R_B)}{L_f} I_b - \frac{1}{L_f} U_{oc}(soc) \quad (2c)$$

$$\frac{d(\mathrm{SOC})}{dt} = \frac{1}{Q_n} I_b \quad (2d)$$

where $u_{\alpha\beta} = \begin{bmatrix} u_\alpha \\ u_\beta \end{bmatrix} = T u_{123}$; $i_{\alpha\beta} = \begin{bmatrix} i_\alpha \\ i_\beta \end{bmatrix} = T i_{123}$; $e_{\alpha\beta} = \begin{bmatrix} e_\alpha \\ e_\beta \end{bmatrix} = T e_{123}$ and T is the $\alpha\beta$ transformation matrix which is given by $T = \sqrt{\frac{2}{3}} \begin{bmatrix} 1 & -\frac{1}{2} & -\frac{1}{2} \\ 0 & \frac{\sqrt{3}}{3} & -\frac{\sqrt{3}}{3} \end{bmatrix}$

For control design purpose, it is more convenient to consider the following averaged model, obtained by averaging the instantaneous model (2a-e) over one switching period (Krein et al., 1990)

$$\dot{x}_{12} = -\frac{r_g}{L_g} x_{12} - \frac{1}{L_g} \mu_{\alpha\beta} x_3 + \frac{1}{L_g} e_{\alpha\beta} \quad (3a)$$

$$\dot{x}_3 = \frac{1}{C_{dc}} \mu_\alpha x_1 + \frac{1}{C_{dc}} \mu_\beta x_2 - \frac{1}{C_{dc}} x_4 \quad (3b)$$

$$\dot{x}_4 = \frac{1}{L_f} x_3 - \frac{(r_f + R_B)}{L_f}\, x_4 - \frac{1}{L_f}\varphi(x_5) \quad (3c)$$

$$\dot{x}_5 = \frac{1}{Q_n} x_4 \quad (3d)$$

where x_1, x_2, x_3, x_4 and x_5 denote the average value of the current i_α, the current i_β, the dc-bus voltage V_{dc}, the battery current I_b and the battery *SOC*, respectively. $\varphi(x_5)$ denotes the open-circuit voltage U_{oc} which is a nonlinear function of the battery *SOC* (See Fig. 3). The control inputs μ_α and μ_β, so-called duty ratio functions, denote the average value of the switching signals u_α and u_β, respectively.

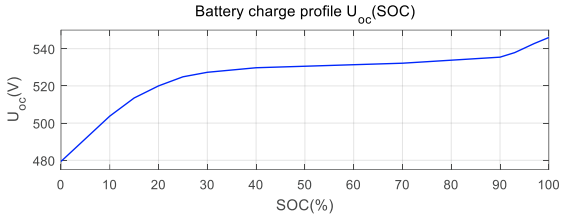

Fig. 3. Battery charge profile $\mathrm{U_{oc}} = \mathrm{f(SOC)}$

After this modeling stage, the focus will be made on the controller design.

3. CONTROLLER DESIGN

The control of the studied system will be implemented to achieve the following objectives: (i) Providing a Unity Power Factor (UPF) during the G2V operating mode; (ii) Regulating the reactive power injected during the V2G operating mode; and (iii) Ensuring the battery charging and the battery discharging, safely.

As the system model (3a-d) is nonlinear, a backstepping design technique is used(Krstić, Kanellakopoulos & Kokotović, 1995; Fadil et al., 2017; Belhaj et al., 2019). To meet all the objectives, the controller design will be developed in two stages: First, two current loops will be designed to ensure the first two objectives, then an outer loop will be performed to achieve the last objective.

3.1 Current Loops Controller Design

The current loops design will be conducted in order to regulate the active power *P* and the reactive power Q to their references P_{ref} and Q_{ref}, respectively. In the PQ theory used in this paper, this goal can be reached by enforcing the two sinusoidal currents $i_\alpha(x_1)$ and $i_\beta(x_1)$ to tracking their references $i_{\alpha_{ref}}(x_{1_{ref}})$ and $i_{\beta_{ref}}(x_{2_{ref}})$, respectively. The relationship is illustrated in the following equations

$$i_{\alpha_{ref}} = \frac{1}{e_\alpha{}^2 + e_\beta{}^2}(P_{ref} e_\alpha - Q_{ref} e_\beta) \quad (4a)$$

$$i_{\beta_{ref}} = \frac{1}{e_\alpha{}^2 + e_\beta{}^2}(P_{ref} e_\beta + Q_{ref} e_\alpha) \quad (4b)$$

Accordingly, let us introduce the following tracking errors

$$z_1 = x_1 - x_{1_{ref}} \quad (5a)$$

$$z_2 = x_2 - x_{2_{ref}} \quad (5b)$$

The control objective is to enforce the errors (z_1, z_2) to vanish. To this end, one needs their dynamics which are obtained, using (5a-b) and (3a), as follows

$$\dot{z}_1 = -\frac{r_g}{L_g} x_1 - \frac{1}{L_g}\mu_\alpha x_3 + \frac{1}{L_g} e_\alpha - \dot{x}_{1_{ref}} \quad (6a)$$

$$\dot{z}_2 = -\frac{r_g}{L_g} x_2 - \frac{1}{L_g}\mu_\beta x_3 + \frac{1}{L_g} e_\beta - \dot{x}_{2_{ref}} \quad (6b)$$

Now, the objective is to make the equilibrium point $(z_1, z_2) = (0,0)$ globally asymptotically stable (GAS). To this end, the following Lyapunov function candidate is chosen

$$V_1 = \frac{1}{2} z_1^2 + \frac{1}{2} z_2^2 \quad (7)$$

Its time derivative $\dot{V}_1 = \dot{z}_1 z_1 + \dot{z}_2 z_2$ can be rendered negative definite by choosing the derivatives of the tracking errors z_1 and z_2 as follows

$$\dot{z}_1 = -c_1 z_1 \quad (8a)$$

$$\dot{z}_2 = -c_2 z_2 \quad (8b)$$

where c_1 and c_2 being positive design parameters.

Indeed, with these choices the derivatives $\dot{V}_1$ becomes

$$\dot{V}_1 = -c_1 z_1^2 + -c_2 z_2^2 \quad (9)$$

which shows that the equilibrium $(z_1, z_2) = (0,0)$ is GAS and, in turn, gives $\lim_{t\to\infty}(z_1, z_2) = 0$. The vanishing of the errors $z_1$and z_2, clearly ensures the active power P regulation and the reactive power Q regulation, respectively.

Combining (6a-b) and (8a-b), the control law μ_α and μ_β are obtained

$$\mu_\alpha = \frac{1}{x_3}(c_1 z_1 L_g - r_g x_1 + e_\alpha - L_g \dot{x}_{1_{ref}}) \quad (10a)$$

$$\mu_\beta = \frac{1}{x_3}(c_2 z_2 L_g - r_g x_2 + e_\beta - L_g \dot{x}_{2_{ref}}) \quad (10b)$$

3.2 SOC Loop Controller Design

The aim, now, is to design a controller which allows imposing the active power reference P_{ref} necessary to ensure the battery charging and battery discharging safely during the G2V and V2G modes, respectively. To do so, the following SOC tracking error is introduced

$$z_3 = x_5 - x_{5_{ref}} \quad (11)$$

Using (3d) and (11) and know that $x_{5_{ref}} = SOC_{ref} = cste$, its dynamics is obtained as follows

$$\dot{z}_3 = \frac{1}{Q_n} x_4 \quad (12)$$

By drawing up an instantaneous power balance transiting from the power grid to the filtering coil, the absorbed power reference P_{ref} can be written as follows

$$P_{ref} = r_g(x_1^2 + x_2^2) + \frac{1}{2} L_g \frac{d}{dt}(x_1^2 + x_2^2) + \frac{1}{2} C_{dc} \frac{d}{dt}(x_3^2) + x_3 x_4 \quad (13)$$

Then the equation (12) becomes

$$\dot{z}_3 = \frac{1}{x_3 Q_n}\Big(P_{ref} - r_g(x_1^2 + x_2^2) - \frac{1}{2}L_g\frac{d}{dt}(x_1^2 + x_2^2) - \frac{1}{2}C_{dc}\frac{d}{dt}(x_3^2)\Big) \quad (14)$$

Now, the objective is to make the equilibrium point ($z_3 = 0$) GAS. For this, the following Lyapunov function candidate is chosen

$$V_2 = \frac{1}{2}z_3^2 \quad (15)$$

its time derivative $\dot{V}_2 = \dot{z}_3 z_3$ can be rendered negative definite by the following choice

$$\dot{z}_3 = -c_3 z_3 \quad (16)$$

where c_3 being a positive design parameter.

Then, the derivative $\dot{V}_2$ becomes

$$\dot{V}_2 = -c_3 z_3^2 \quad (17)$$

Finally, combining (16) and (14), the reference P_{ref} of the current loop is obtained

$$P_{ref} = -c_3 z_3 x_3 Q_n + r_g(x_1^2 + x_2^2) + \frac{1}{2}L_g\frac{d}{dt}(x_1^2 + x_2^2) + \frac{1}{2}C_{dc}\frac{d}{dt}(x_3^2) \quad (18)$$

The main result of this subsection is summarized in the following Theorem.

Theorem 1. Consider the Single-Stage V2G Three-Phase BEV Charger system illustrated in Fig. 2 and described by its nonlinear model (3a-d) in the closed-loop with the nonlinear controller represented by the control laws (10a), (10b) and (18), then, one has the following properties

1) Using (8a), (8b) and (16), one can easily check that the tracking errors vector $z = [\,z_1 \quad z_2 \quad z_3]^t$ undergoes the following equation

$$\dot{z} = \Phi z \quad (19)$$

with

$$\Phi = \begin{pmatrix} -c_1 & 0 & 0 \\ 0 & -c_2 & 0 \\ 0 & 0 & -c_3 \end{pmatrix}$$

It follows that the vector z is a GAS system which means that all tracking errors converge exponentially to zero whatever the initial conditions;

2) The tracking error z_1 vanishes exponentially implying that the active power tuning objective is achieved;

3) The tracking error z_2 goes exponentially ensuring the reactive power regulation;

4) The tracking error z_3 decays exponentially to zero ensuring the battery charging and the battery discharging safely.

Proof: One can readily check that the matrix Φ is Hurwitz, which means that the closed-loop system (19) is GAS. This ends the proof of the theorem.

4. SIMULATION RESULTS AND DISCUSSIONS

In this section, the aim is to improve the effectiveness of the proposed PQ theory-based nonlinear controller. Accordingly, many numerical simulations are performed using the MATLAB/Simulink software and the obtained results are illustrated in Fig. 5 to Fig. 7. To this end, the instantaneous model (1a-d) is used for modeling the studied system while the averaged model (3a-d) is only using for controller design. The simulation workbench is illustrated in Fig. 4 while the system parameters are listed in Table 1.

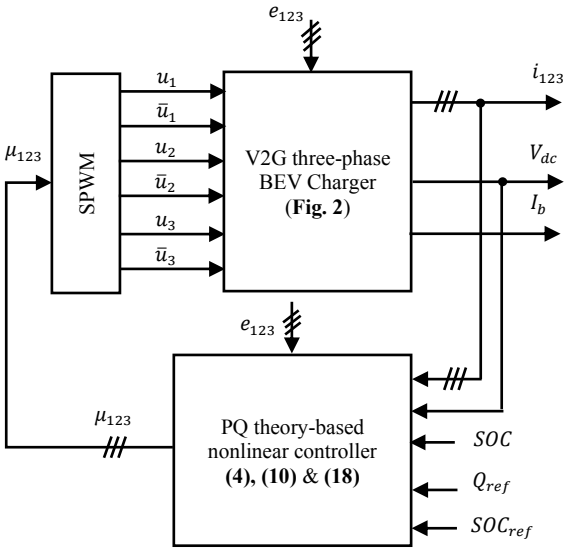

Fig. 4. Simulation workbench of the V2G single-stage three-phase charger

Table 1. System Parameters

Parameter	Symbol	Value
Grid phase-neutral voltage	**E**	230V
Power grid frequency	**f**	50Hz
Grid-side Inductor	$\mathbf{L_g}$, $\mathbf{r_g}$	5mH, 0.1Ω
Switching frequency	$\mathbf{F_S}$	20KHz
DC-Bus Capacitor	$\mathbf{C_{dc}}$	2000μF
Battery-side Inductor	$\mathbf{L_f}$, $\mathbf{r_f}$	1.5mH, 0.1Ω
Battery ESR	$\mathbf{R_B}$	0.06Ω
Battery Capacity	$\boldsymbol{Q_n}$	40Ah
Design parameters	$\mathbf{c_1}$	1 000 000
	$\mathbf{c_2}$	100 000
	$\mathbf{c_3}$	10
	$\mathbf{T_d}$	0.0001

All of the simulation results, shown in Fig. 5 to Fig. 7, clearly illustrate that all the objectives of the proposed controller are achieved. Indeed, Fig. 5a-e illustrate the PQ theory-based controller performances during V2G operating mode. Fig. 5a shows the sinusoidal three-phase power grid voltages e_1, e_2 et e_3 while the Fig. 5b illustrates clearly that the three-phase power grid currents i_1, i_2 and i_3 are sinusoidal. Fig. 5c shows that the grid current $i_1$is sinusoidal and in phase with the grid voltage v_1. This result is the satisfaction of the UPF objective in the grid-side. Fig. 5d shows that the control laws μ_1, μ_2, and μ_3 are sinusoidal and bounded between 0 and 1. Fig. 5e illustrates that the battery voltage V_b is an increasing time function which

fulfilling the G2V charging objective. At the charging end, exactly at time 0.7h, the battery voltage V_b shows a discontinuity due to the voltage drop across the battery ESR. Fig. 5f illustrates the battery current I_b time-variation which shows clearly that the battery charging is carried out using the constant-current (CC) process with 1C (C-rate is a current rate normalized to battery nominal capacity in this work 1C ➔ 40A). Fig. 5g shows the voltage U_{oc} which evolves identically to the voltage V_b. Finally, Fig. 5h represents the battery SOC which linearly increases (Constant-Current process charging) by 30% to 100%. This proves that the battery is charging.

On the other hand, all of the curves shown in Fig. 6 illustrate that the energy flows from EV battery to the power grid correctly and all of the controller objectives in V2G operating mode are reached. The grid current i_1 still sinusoidal but in phase opposition with the power grid voltage v_1(Fig. 6c). The battery is discharging with a negative constant current I_b (Fig. 6f) and the battery SOC decreases from 100% to 30% (Fig. 6h). This proves that the V2G mode is then activated and that the whole studied system {combining the EV battery and the bidirectional three-phase charger} is injecting active energy into the power grid.

To substantiate that the reactive power regulation objective in V2G mode is achieved, a simulation was performed in the presence of injected reactive power step changes. Thus, Fig. 7a-b, illustrate that the grid current i_1 and the grid voltage v_1 are in phase opposition which means that the studied bidirectional charger operates in V2G mode without injecting a reactive power. Fig. 7c-d clearly show that the charger also operates in V2G mode but with injecting a 22Kvar reactive power.

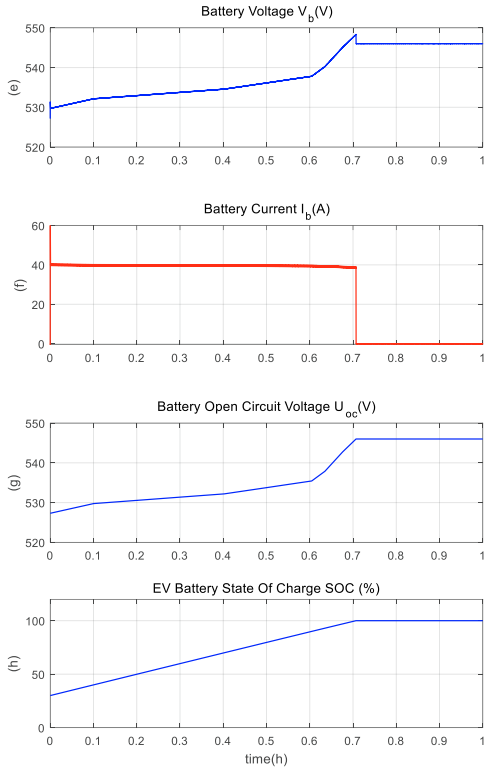

Fig. 5. PQ theory-based controller performances during G2V mode

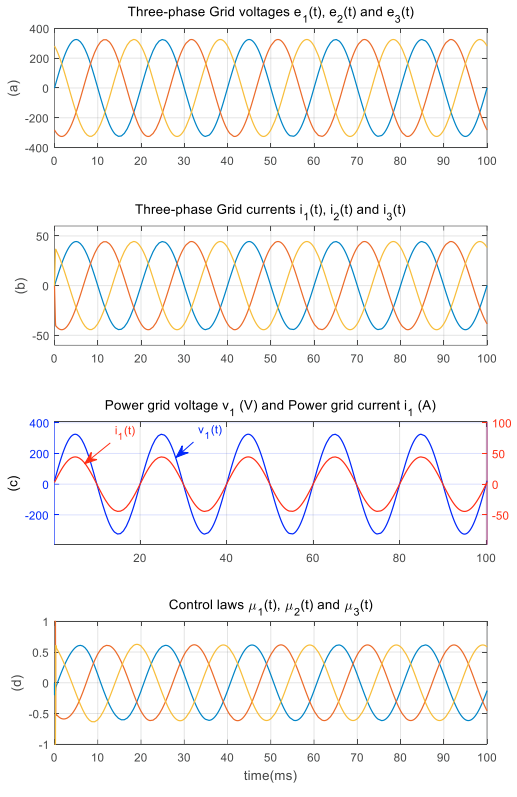

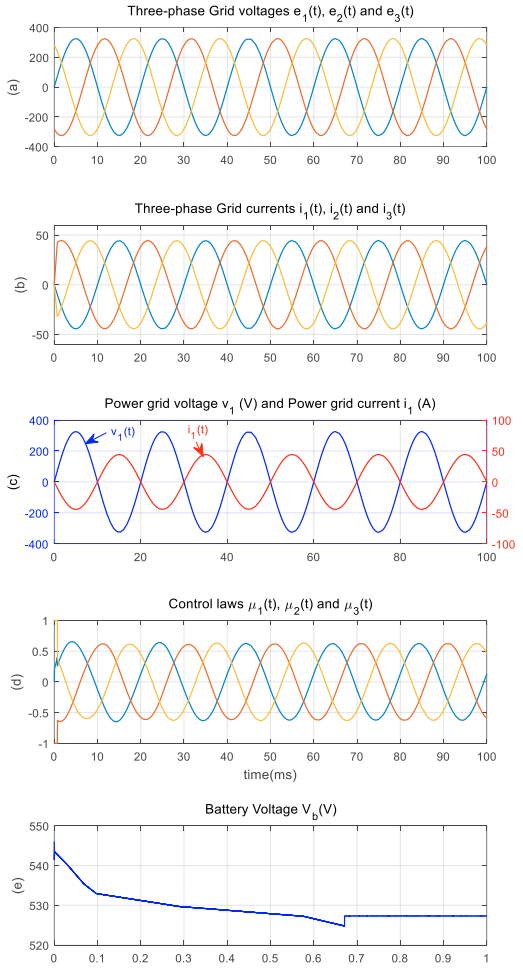

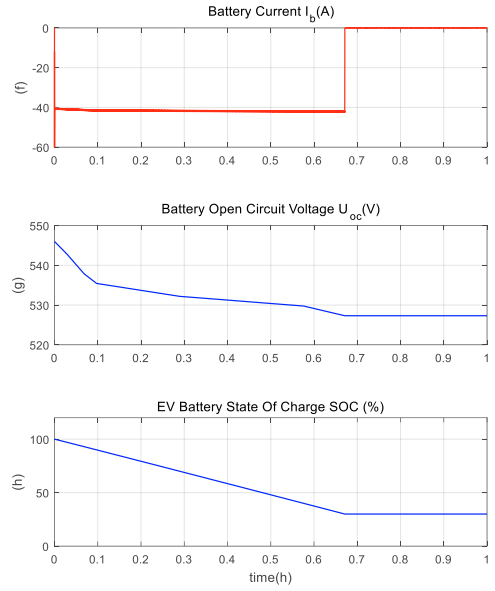

Fig. 6. Controller performances during V2G operating mode

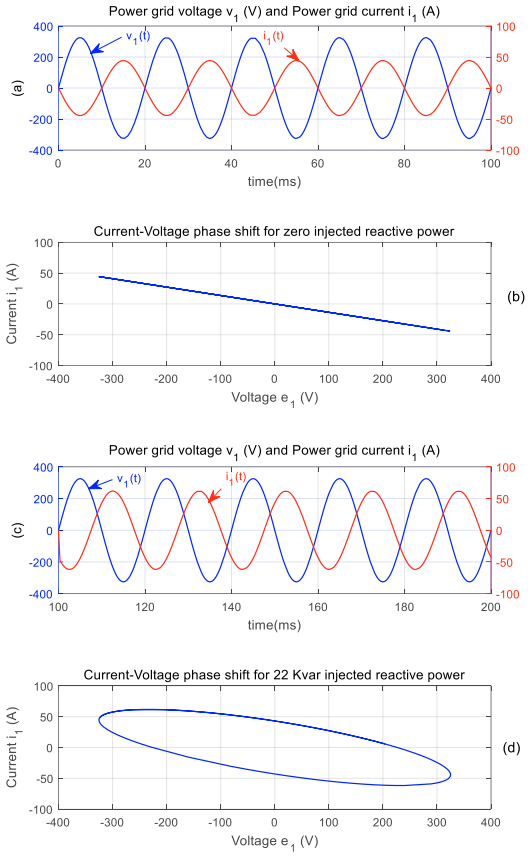

Fig. 7. Controller performances in the presence of injected reactive power step changes

5. CONCLUSION

In this work, the problem of controlling V2G single-stage three-phase BEV charger has been addressed. Accordingly, a nonlinear controller was designed in order to meet all control objectives namely: (i) Unity power factor during the G2V operating mode; (ii) Injected reactive power regulation during the V2G operating mode; and (iii) Battery charging and battery discharging during the G2V mode and V2G mode, respectively. It consisted of a multi-loops structure using the backstepping technique and the PQ theory. Theoretical analysis and numerical simulations have clearly illustrated that all control objectives are achieved.

ACKNOWLEDGMENT

The authors gratefully acknowledge the support of the Moroccan Ministry of Higher Education (MESRSFC) and the CNRST under grant PPR/2015/36.

REFERENCES

Anon (2017). Battery Modeling. In: *Hybrid Electric Vehicles*. Chichester, UK, John Wiley & Sons, Ltd,2017:371–383.

Belhaj FZ et al. (2019). Output feedback control of supercapacitors parallel charging system for EV applications: Theoretical design and experimental validation. *International Journal of Adaptive Control and Signal Processing*, 33(9):1374–1394.

Buja G, Bertoluzzo M, Fontana C (2017). Reactive Power Compensation Capabilities of V2G-Enabled Electric Vehicles. *IEEE Transactions on Power Electronics*, 32(12):9447–9459.

El Fadil H et al. (2017). Nonlinear Modeling and Observer for Supercapacitors in Electric Vehicle Applications. *IFAC-PapersOnLine*, 50(1):1898–1903.

Krein PT et al. (1990). On the use of averaging for the analysis of power electronic systems. *IEEE Transactions on Power Electronics*, 5(2):182–190.

Krstić M, Kanellakopoulos I, Kokotović PV (1995). *Nonlinear and adaptive control design*. New York, Wiley.

Mahmud K et al. (2018). Integration of electric vehicles and management in the internet of energy. *Renewable and Sustainable Energy Reviews*, 82:4179–4203.

Mi C, Masrur MA (2017). *Hybrid Electric Vehicles: Principles and Applications with Practical Perspectives*. Wiley (Automotive Series - Wiley).

Rachid A et al. (2017). Lyapunov-based control of single-phase AC-DC power converter for BEV charger. *3rd International Conference on Electrical and Information Technologies (ICEIT)*. Rabat, Morocco.

Rachid A et al. (2019a). Nonlinear output feedback control of V2G single-phase on-board BEV charger. *Asian Journal of Control*:1–12. https://doi.org/10.1002/asjc.2082

Rachid A et al. (2019b). Advanced Control of Three-Phase Battery Electric Vehicle Charger with V2X technology. *Int. J. Modelling, Identification and Control*. In press.

Rachid A, El Fadil H, Giri F (2018). Dual Stage CC-CV Charge Method for Controlling dc-dc Power Converter in BEV Charger. *19th IEEE Mediterranean Electrotechnical Conference (MELECON)*. Marrakesh, Morocco.

Rubino L, Capasso C, Veneri O (2017). Review on plug-in electric vehicle charging architectures integrated with distributed energy sources for sustainable mobility. *Applied Energy*, 207:438–464.

Yilmaz M, Krein PT (2013). Review of Battery Charger Topologies, Charging Power Levels, and Infrastructure for Plug-In Electric and Hybrid Vehicles. *IEEE Transactions on Power Electronics*, 28(5):2151–2169.